DIABETES/METABOLISM RESEARCH AND REVIEWS
Diabetes Metab Res Rev 2004; **20**: 61–71.
Published online in Wiley InterScience (www.interscience.wiley.com). **DOI:** 10.1002/dmrr.421

RESEARCH ARTICLE

The role of the sodium hydrogen exchanger-1 in mediating diabetes-induced changes in the retina

Mark Cukiernik[1]
Denise Hileeto[1]
Donal Downey[2]
Terry Evans[1]
Zia Ali Khan[1]
Morris Karmazyn[3]
Subrata Chakrabarti[1,4]*

[1]*University of Western Ontario, Department of Pathology, Canada*

[2]*University of Western Ontario, Department of Diagnostic Radiology, Canada*

[3]*University of Western Ontario, Department of Physiology & Pharmacology, Canada*

[4]*University of Western Ontario, Department of Microbiology & Immunology, Canada*

*Correspondence to: Dr Subrata Chakrabarti, University of Western Ontario, Department of Pathology, Dental Sciences Building, London, Ontario, N6A 5C1, Canada. E-mail: schakrab@uwo.ca

Received: 30 May 2003
Revised: 22 September 2003
Accepted: 2 October 2003

Abstract

Background The sodium hydrogen exchanger (NHE) is a transmembrane protein responsible for alkalinization and control of intracellular acidosis by the removal of hydrogen and the subsequent influx of sodium. Our investigation attempts to determine the role of NHE-1 in the pathogenesis of early retinal microangiopathy due to diabetes.

Methods Diabetes was induced in male Sprague–Dawley rats with a single intravenous streptozotocin injection (65 mg/kg). To examine the duration-dependent changes in NHE-1 expression, retinas from 1-, 6- and 12-week diabetic animals were analyzed. To examine the functional consequences of NHE-1 inhibition in comparison with good blood glucose control, diabetic rats were randomly assigned to poorly controlled diabetic, well-controlled diabetic, poorly controlled diabetic with cariporide groups and were compared with nondiabetic controls after six weeks. Cariporide is an orally active inhibitor of NHE-1 (6000 ppm in rat chow). At the end of the treatment period, color Doppler ultrasound was used to determine the resistivity index (RI) of the central retinal artery. The mRNA expression of endothelin (ET) isoforms 1 and 3, inducible and endothelial nitric oxide synthase (iNOS and eNOS respectively) and NHE-1 were examined. NHE-1 distribution was localized with immunohistochemistry.

Results All diabetic animals showed hyperglycemia, increased glycated hemoglobin and lower body weight gain compared to nondiabetic controls. Diabetes caused an increased RI, indicative of retinal vasoconstriction, which was corrected by both cariporide treatment and good glucose control. NHE-1 was localized in the endothelium of the retinal microvasculature and the neuronal and glial components. NHE-1 mRNA expression was unchanged after 1 week and increased after 6 and 12 weeks of diabetes. Furthermore, a diabetes-induced upregulation of ET-1 and ET-3 mRNA expression after six weeks was corrected with cariporide treatment. NHE-1 inhibition of diabetic animals upregulated iNOS mRNA levels, although expression of eNOS and iNOS mRNA were not altered in poorly controlled diabetes. Improved blood glucose control with higher doses of insulin also corrected diabetes-induced increased RI by upregulating eNOS and iNOS mRNA expression.

Conclusions The results of the study suggest that NHE-1 may be involved in the regulation of several vasoactive modulators that contribute to functional alterations in diabetic retinal microangiopathy. Copyright © 2004 John Wiley & Sons, Ltd.

Keywords retina; sodium hydrogen exchanger-1; endothelin; nitric oxide synthase

Introduction

The sodium hydrogen exchanger (NHE) represents a family of eight proteins responsible for the removal of intracellular hydrogen ions and concomitant influx of sodium ions [1–3]. The 815 amino acid residue protein, of approximately 110 kDa is made up of an N-terminus transmembrane channel and a C-terminus regulatory region [4]. Isoform 1 (NHE-1) is considered to be ubiquitously expressed and is found in virtually all tissues [5]. Intracellular hydrogen ion concentration is one of the main stimuli leading to NHE activation. However, other factors that act as important mediators of chronic diabetic complications, such as Protein Kinase C (PKC) and endothelins (ETs) may act as NHE activators [4,6,7]. Along with pH maintenance, NHE-1 is involved in several other physiological processes such as cell adhesion and cell growth [8].

Diabetic retinopathy is a disease involving the microvasculature of the retina [9]. Several biochemical pathways are activated, which lead to tissue damage. These systems include activation of PKC, activation of the polyol pathway, formation of advanced glycation end (AGE) products, oxidative stress and the upregulation of proinflammatory cytokines and vascular modulators [10]. Two early vascular modulators are ETs and nitric oxide (NO) [11]. Both ET and NO are involved in the regulation of retinal blood flow in diabetes [12]. We have previously demonstrated that diabetes-induced retinal vasoconstriction is mediated by ETs [13,14]. We have shown that ETs are involved with increased fibronection and collagen production [15] and capillary basement membrane thickening in the retina, heart and kidney via NF kappa B and AP-1 activation [15–17].

In the heart, we found that some of the effects of ETs may be mediated via NHE-1 [18,19]. NHE-1 may modulate blood flow by virtue of its regulatory interaction with ET-1 [20–23]. We have further demonstrated an amelioration of diabetic cardiomyopathy with the use of a specific NHE-1 inhibitor cariporide [18]. Furthermore, it has been demonstrated that NHE-1 plays an important role in the pathogenesis of diabetic nephropathy [24–26]. Although NHE-1 activity has previously been demonstrated in the retinal photoreceptor and pigment epithelium [27–29], a possible alteration of NHE-1 and its functional consequences in diabetes has not been studied in the retina.

Exogenous insulin may act as a growth factor leading to the activation of cellular pathways like mitogen-activated protein kinase (MAPK), and the upregulation of several molecules like ETs, NO Synthase (NOS) and NHE-1 [30–32]. With respect to the diabetic heart, insulin has been demonstrated to increase both the expression and activity of NHE-1 [33]. However, NHE-1 expression has not been studied in the diabetic retina. Hence, in this study, we investigated the diabetes-induced changes of NHE-1 in the rat retina, its effects on vasoactive factors and their functional consequences. We used a specific NHE-1 inhibitor cariporide to investigate diabetes-induced transcriptional changes and blood flow alterations and compared its effects with animals either with poor or improved glucose control with higher doses of insulin.

Materials and methods

Animals

All animals were cared for under the conditions and rules designated by the ARVO Statement for the Use of Animals in Ophthalmic and Vision Research with approval by the University of Western Ontario Animal Care and Ethics Committee. Male Sprague Dawley rats of approximately 200 g received a single intravenous injection of streptozotocin (65 mg/kg in citrate buffer, pH = 5.6). Control animals received an equal volume injection of citrate buffer. After confirmation of diabetes (blood glucose >20 mmol/L on two consecutive days), animals were randomized to the various treatment groups ($n = 5$): Poorly controlled diabetes, poorly controlled diabetes treated with cariporide (6000 ppm in rat chow) and well-controlled diabetes. To examine the duration-dependent alterations of NHE-1 mRNA expression in the retina in diabetes, nondiabetic and poorly controlled diabetic animals were sacrificed after 1, 6 and 12 weeks of follow-up. The functional effects of cariporide treatment were compared with good blood glucose control after six weeks of diabetes due to the upregulation of NHE-1 at this time point. Animals were fed with rat chow and water *ad libitum*. Animals were monitored for body weight changes, glucosuria and ketouria. All diabetic rats were implanted with slow release insulin implants to prevent ketosis (approx 2 U/day) (LinShin. Scarborough, ON, Canada). Well-controlled diabetic animals were implanted with two slow release implants (approx 4 U/day). Cariporide, (courtesy Dr. A. Busch, Aventis Pharma, Frankfurt Germany) is a selective NHE-1 inhibitor [34]. Cariporide treatment started after the confirmation of diabetes and was continued for the whole treatment period. The animals were killed and the retinal tissue was either snap frozen in liquid nitrogen or preserved in 10% buffered formalin solution. Blood was collected for glucose (LifeScan, Burnaby, BC, Canada) and glycated hemoglobin (Sigma Aldrich Canada, Oakville ON Canada) measurements.

Color Doppler ultrasound

Prior to sacrifice, color Doppler ultrasound analysis of the right eye was performed in animals with six weeks of follow-up using previously described techniques. Briefly, following ketamine and xylazine anesthesia, the central retinal vasculature was located with an 8L5, 80-MHz color Doppler ultrasound probe (Acuson Mountainview, CA, USA). Doppler waveforms were examined and

color images were obtained in real time with Doppler spectral analysis using the arterial tracings. At least three measurements were recorded for each animal and the mean was calculated. The resistivity index (RI) of the central retinal artery was calculated by subtracting the diastolic velocity (DV) from the peak systolic velocity (SV) and dividing by the systolic velocity [(SV − DV) ÷ SV]. An increased central retinal artery RI value is indicative of vasoconstriction at the capillary or pre-capillary level within the retina.

RNA isolation

Using TRIZOL™ reagent (Invitrogen Inc. Burlington, ON, Canada), RNA was extracted as previously described [18].

First-strand cDNA synthesis

Using the Superscript-II system (Invitrogen Inc.), first-strand cDNA was made using four micrograms of RNA as previously described [18].

Competitive RT PCR

Owing to its quantitative capabilities, competitive RT PCR was used to quantify the expression of the specific mRNAs as previously described [18]. Briefly, heterologous competitors were created with the TaKaRa DNA Competitor Construction Kit (Panvera, Madison WI, USA) as per manufacturer's instructions. Amplification was performed with the sense (S) and anti-sense (AS) primers found in Table 1. For all primer sets, 1× PCR buffer, 1.0 μL RT product, 2.5 μL of the appropriate dilution of competitor, 500 nM of sense and anti-sense primer, 0.25 mM of dNTP and 2.5 U of Platinum Taq™ (Invitrogen Inc.) along with 2.0 mM $MgCl_2$ for NHE-1, ET-1, ET-3 or 1.5 mM $MgCl_2$ for eNOS, iNOS to a final volume of 25 μL. 35 cycles of amplification were used for ET-3 amplification and all other genes amplified with 30 cycles; 92 °C for 45 s, 60 °C for 45 s and 72 °C for 1 min, followed by a final extension of 72 °C for 10 min. Preliminary experiments confirmed that amplification was in the linear phase of the PCR reaction.

Quantification

The PCR products were analyzed on a 3% agarose gel in a 1× TRIS borate EDTA (TBE) buffer. The gels were stained with ethidium bromide and visualized with ultraviolet light. For quantification, the ratio of density and area of the target gene band and its competitor band were assessed using Mocha™ densitometry software (Jandel Scientific, CA, USA). As the target and competitor DNA

Table 1. Primer sequences and LightCycler parameters

Primer sequence Sense: 5′ → 3′ Anti-sense: 5′ → 3′	PCR parameters (temperature & time, ramp rate) Denaturation (D), Annealing (A), Extension (E), Signal Acquisition (S), # of cycles (#)	Melting curve analysis (temperature & time, ramp rate)
ET-1	D: 95 °C (0 s) 20 °C/s A: 58 °C (5 s) 20 °C/s	Step 1: 95 °C (0 s) 20 °C/s Step 2: 63 °C (15 s) 20 °C/s
S: GCTCCTGCTCCTCCTTGATG AS: CTCGCTCTATGTAAGTCATGG	E: 72 °C (20 s) 20 °C/s S: 84 °C (1 s) 20 °C/s #: 40	Step 3: 95 °C (0 s) 0.1 °C/s Signal: Continuous
ET-3	D: 95 °C (0 s) 20 °C/s A: 58 °C (5 s) 20 °C/s	Step 1: 95 °C (0 s) 20 °C/s Step 2: 65 °C (15 s) 20 °C/s
S: GCACTTGCTTCACTTATAAGG AS: CAGAAGCAAGAAGCATCAGTTG	E: 72 °C (17 s) 20 °C/s S: 84 °C (1 s) 20 °C/s #: 55	Step 3: 95 °C (0 s) 0.1 °C/s Signal: Continuous
eNOS	D: 95 °C (0 s) 20 °C/s A: 57 °C (5 s) 20 °C/s	Step 1: 95 °C (0 s) 20 °C/s Step 2: 67 °C (15 sec) 20 °C/s
S: CAAGACCGATTACACGACA AS: GTCCTCAGGAGGTCTTGCAC	E: 72 °C (9 s) 20 °C/s S: 85 °C (1 s) 20 °C/s #: 45	Step 3: 95 °C (0 s) 0.1 °C/s Signal: Continuous
iNOS	D: 95 °C (0 s) 20 °C/s A: 57 °C (5 s) 20 °C/s	Step 1: 95 °C (0 s) 20 °C/s Step 2: 67 °C (15 s) 20 °C/s
S: ATGGAACAGTATAAGCGAAACACC AS: GTTTCTGGTCGATGTCATGAGCAAAGG	E: 72 °C (9 s) 20 °C/s S: 84 °C (1 s) 20 °C/s #: 45	Step 3: 95 °C (0 s) 0.1 °C/s Signal: Continuous
NHE-1	D: 95 °C (0 s) 20 °C/s A: 57 °C (5 s) 20 °C/s	Step 1: 95 °C (0 s) 20 °C/s Step 2: 67 °C (15 s) 20 °C/s
S: TCTGTGGACCTGGTGAATGA AS: GTCACTGAGGCAGGGTTGTA	E: 72 °C (9 s) 20 °C/s S: 84 °C (1 s) 20 °C/s #: 45	Step 3: 95 °C (0 s) 0.1 °C/s Signal: Continuous
β Actin	D: 95 °C (0 s) 20 °C/s A: 58 °C (5 s) 20 °C/s	Step 1: 95 °C (0 s) 20 °C/s Step 2: 67 °C (15 s) 20 °C/s
S: CCTCTATGCCAACACAGTGC AS: CATCGTACTCCTGCTTGCTG	E: 72 °C (8 s) 20 °C/s S: 83 °C (1 s) 20 °C/s #: 35	Step 3: 95 °C (0 s) 0.1 °C/s Signal: Continuous

to be amplified use the same primers, the ratio between the two amplified products reflects the original amounts of target DNA and competitor.

Real-time PCR

To confirm results obtained using competitive PCR, real-time quantitative PCR with the Roche LightCycler system (Roche Diagnostics Canada, Lavalle PQ Canada) was used. By using the SYBR green detection system, the products' amplification and detection occurred in a single reaction tube. PCR reactions were performed in micro capillary tubes (Roche Diagnostics Canada) to a final volume of 20 µL. The reaction mixture was made from 2.0 µL DNA-SYBR mix [Lightcycler FastStart enzyme and Reaction Mix SYBR green I] (Roche Diagnostics Canada), 1.6 µL of 25 mM $MgCl_2$, 1.0 µL of 10 µM sense and antisense primers, 13.4 µL of PCR grade water and 1.0 µL of cDNA template. All primers' sequences and PCR profiles are listed in Table 1. For all genes listed, prior to the initiation of the PCR cycles, 1 cycle of 94 °C for 10 min was used to activate the FastStart DNA polymerase. To optimize the amplification of the genes, melting curve analysis (MCA) was used to determine the melting temperature (T_m) of specific products and primer-dimers. According to the T_m value of specific products, an additional step (signal acquisition step, 2–3 °C below T_m) was added following the elongation phase of RT PCR. This additional step in the PCR reactions allowed for signal acquisition from specific target products. mRNA was quantified with the standard curve method. Standard curves were constructed using different amounts of standard template. The cycle number, C_p (crossing point), which produces a significantly different fluorescence signal from baseline was used to compute the relative concentration of the target genes from the standard curves. The data was normalized to ß-actin in order to account for differences in reverse transcription efficiencies and template amounts within each sample.

Immunocytochemistry

Five-micrometer tissue sections from formalin-fixed, paraffin-embedded blocks that were transferred to positively charged slides were used for staining. A polyclonal rabbit antirat NHE-1 antibody (Chemicon International Inc, Temecula CA, USA) (1 : 50) was used along with the streptavidin biotin reaction (Vectastain Elite Kit, Vector Laboratories. Burlingame, CA, USA). Diaminobenzidine was used as a chromogen. Slides were counterstained with hematoxylin. For negative controls, the primary antibody was replaced with nonimmune rabbit serum. The experiments were repeated in triplicate with slides analyzed in a masked fashion by two investigators. Slides were described specifically to the localization of staining within the retinal layers.

Statistical analysis

All values are displayed as mean ± SEM. Values were analyzed with ANOVA and Fisher's exact test. A p-value of 0.05 or less was considered significant.

Results

Clinical monitoring

Poorly controlled diabetic animals demonstrated increased blood glucose levels, decreased weight gain and high glycated hemoglobin levels (Table 2). Treatment with cariporide did not affect any of these parameters. Animals with improved blood glucose control demonstrated better body weight gain, yet the weights were lower than nondiabetic control animals. With respect to both blood glucose and glycated hemoglobin, well-controlled diabetic animals demonstrated levels significantly different from both poorly controlled diabetes and nondiabetic control animals suggesting that a partial effect was achieved (Table 2).

Diabetes-induced increased retinal resistivity index is associated with higher ET and NHE-1 mRNA expression

Poorly controlled diabetes demonstrated an increased resistivity index as compared to nondiabetic control animals (Figure 1). The increases in RI are associated with an increase in both ET-1 and ET-3 mRNA levels (Figure 2) as well as increased NHE-1 mRNA (Figure 3(b)). Analysis of NHE-1 mRNA in a duration-dependent manner determined that NHE-1 mRNA was not upregulated

Table 2. Clinical monitoring of data after six weeks of diabetes

Treatment	Body weight (*g*)	Blood glucose (mmol/L)	Glycated hemoglobin (%)
Nondiabetic control	526 ± 11.11	4.87 ± 0.17	6.70 ± 0.77
Poorly controlled diabetes	458 ± 14.95*	19.67 ± 1.37*	13.78 ± 0.63*
Well-controlled diabetes	482 ± 18.38*	9.40 ± 1.61*[a]	8.83 ± 0.55*[a]
Poorly controlled diabetes with cariporide	443 ± 19.14*	15.43 ± 1.55*	12.13 ± 0.45*

Data is displayed as mean ± SEM.
*Denotes significant difference from nondiabetic control.
[a]Denotes significant difference from poorly controlled diabetes.

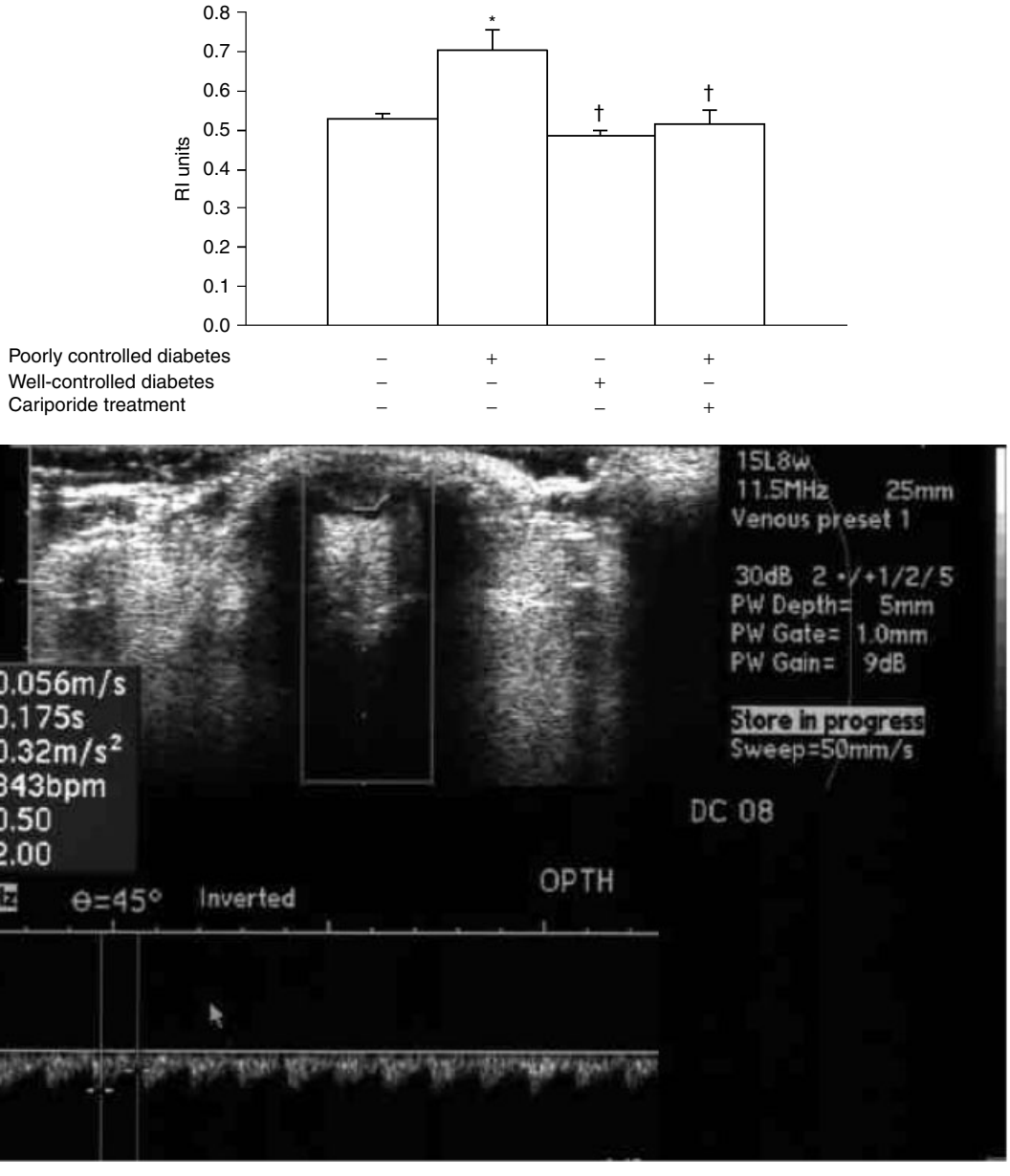

Figure 1. Resistivity index (RI) of the central retinal artery. The upper panel represents the analysis of the mean RI values ± SEM. The lower panel is a representative color Doppler ultrasound image. RI is calculated from the arterial tracing (please see materials and methods) (* significantly different from nondiabetic control, † significantly different from poorly controlled diabetes. $n = 5$ for all groups)

at one week. However, NHE-1 mRNA was elevated at 6 weeks and remained elevated after 12 weeks of diabetes (Figure 3(a)). Both ET-1 and ET-3 can act as vasoconstrictor peptides through an interaction with the ET type A receptor [11,12]. NOS, on the other hand, through the production of NO may stimulate vasodilation [11]. It should be noted that eNOS and iNOS mRNA levels were not altered because of diabetes (Figure 4).

NHE-1 inhibition with cariporide prevented a diabetes-induced increased RI and ET expression

Treatment of poorly controlled diabetic animals with cariporide prevented the diabetes-induced increased RI (Figure 1). NHE-1 mRNA expression was significantly increased in the retina of poorly controlled diabetic animals (Figure 3(a)). To further confirm our data, we used real-time PCR, which agreed with the data obtained by competitive PCR. A diabetes-induced increase in ET-1 and ET-3 mRNA transcription was attenuated with cariporide treatment (Figure 2). NHE-1 inhibition also increased the transcription of iNOS mRNA whereas eNOS remained unchanged (Figure 4).

Well-controlled diabetes prevents RI increases via NOS

Good glucose control improved the diabetes-induced increase in the resistivity index (Figure 1). The

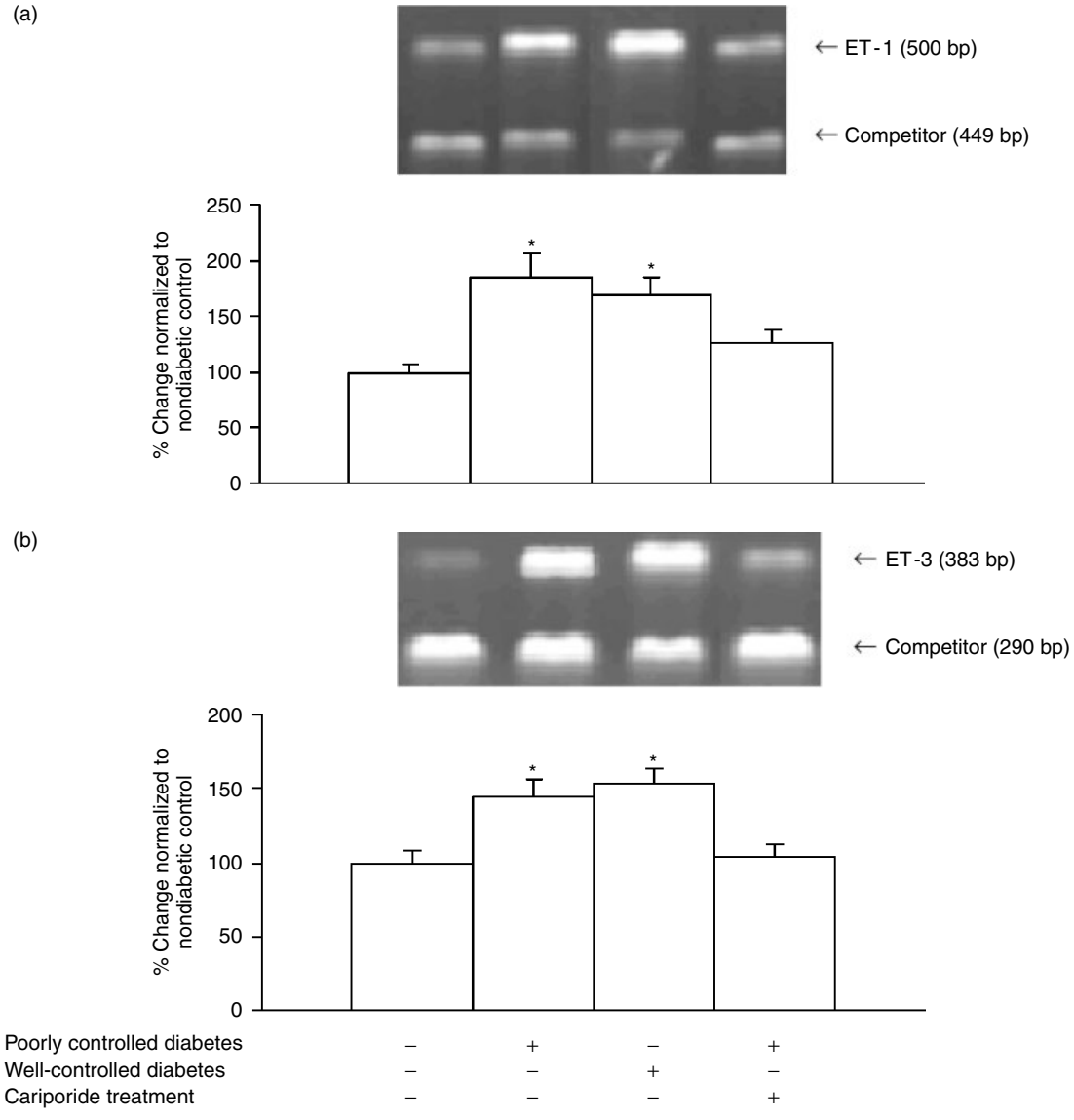

Figure 2. Endothelin 1 and 3 mRNA expression. (a) Endothelin-1 (ET-1) mRNA expression showing that diabetes-induced increased expressions were corrected by cariporide treatment. (b) Endothelin-3 (ET-3) mRNA expression in the retina. The upper panels of both parts (a) and (b) are representative gel pictures obtained from competitive RT PCR. Similar data were obtained with real-time PCR analysis. (∗ significantly different from nondiabetic control. $n = 5$ for all groups)

improvement in RI was associated with increased eNOS and iNOS mRNA levels (Figure 4). However, no effect of good glucose control was seen on diabetes-induced increased ET-1 and ET-3 mRNA transcription (Figure 2). On the other hand, good blood glucose control increased NHE-1 mRNA expression (Figure 3(b)).

NHE-1 is localized in the retina

Immunocytochemically, NHE-1 was seen in the ganglion cells, photoreceptor outer segments as well as in the endothelial cells of the microvasculature. The arborizing fibers of the inner plexiform layer also stained positively, suggesting possible immunoreactivity in the glial fibers (Figure 5). Localization was predominantly at the cell membrane. No immunoreactivity was seen in the negative controls (Figure 5). Immunoreactivity was increased in the retina of diabetic animals in keeping with mRNA expression (Figure 5).

Discussion

The present study demonstrates that NHE-1 plays a role in diabetes-induced vasoconstriction in the retina. Such changes may be mediated through ET and NOS. We found that NHE-1 is present in the retina, both in the neuronal tissue as well as in the endothelial cells. No NHE-1 immunoreactivity was seen within the pericytes. Previous reports have documented the presence of NHE-1 within the retinal pigment epithelium, the ciliary body, the cornea and cultured endothelial cells isolated from large vessels [35–39].

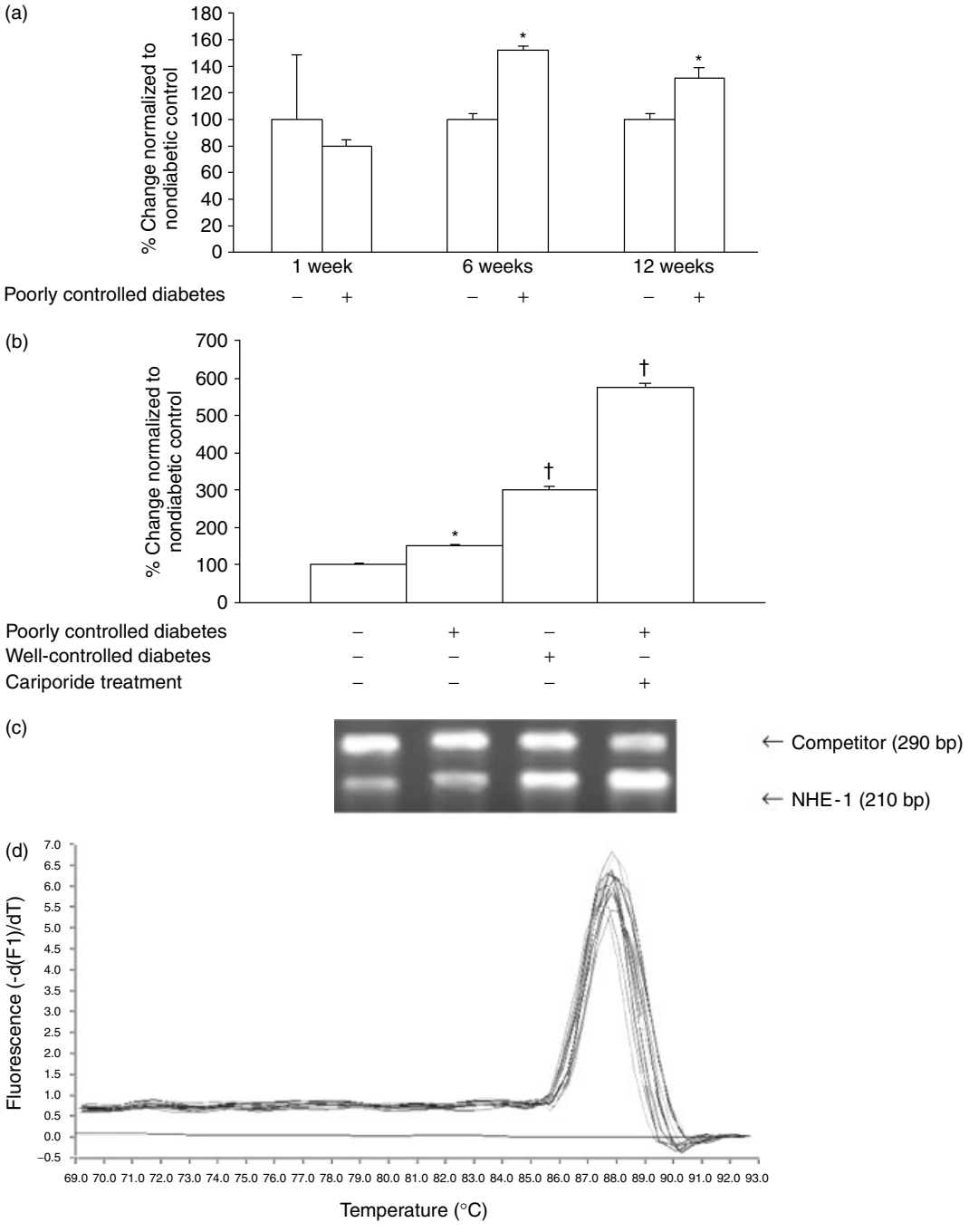

Figure 3. NHE-1 mRNA expression. (a) Represents duration-dependent alteration of NHE-1 mRNA expression after 16 and 12 weeks of diabetes in the retina. (b) Represents NHE-1 mRNA levels in various treatment groups after six weeks of diabetes and (c) is a representative competitive PCR gel picture of the treatment groups described in (b). Similar data were obtained with real-time PCR. (d) Represents melting curve analysis, demonstrating the specificity of amplification where all samples showed a specific product with T_m of 88 °C. (∗ = significantly different from nondiabetic controls † = significantly different from poorly controlled diabetes, $n = 5$ for all groups)

This is the first demonstration of increased NHE-1 mRNA expression in the retina in diabetes. In this study, two sets of PCR techniques (real time and competitive) were used to confirm the increased retinal expression of NHE-1 mRNA. Several factors may lead to increased retinal NHE-1 mRNA expression in diabetes including AGE accumulation, MAPK activation, PKC activation, and oxidative stress as previously demonstrated by other investigators [7,40–42]. Increased NHE-1 mRNA has been demonstrated in the kidney of diabetic animals [43] and increased erythrocyte NHE activity has been correlated with the development of nephropathy in type 1 diabetes [44]. Lymphocytes from diabetic patients with nephropathy and hypertension show increased NHE activity [45]. In this study, short-term diabetes did not elevate NHE-1 mRNA expression, which was elevated after 6 weeks and remained so after 12 weeks. In animal diabetes, the aorta from diabetic rats show increased

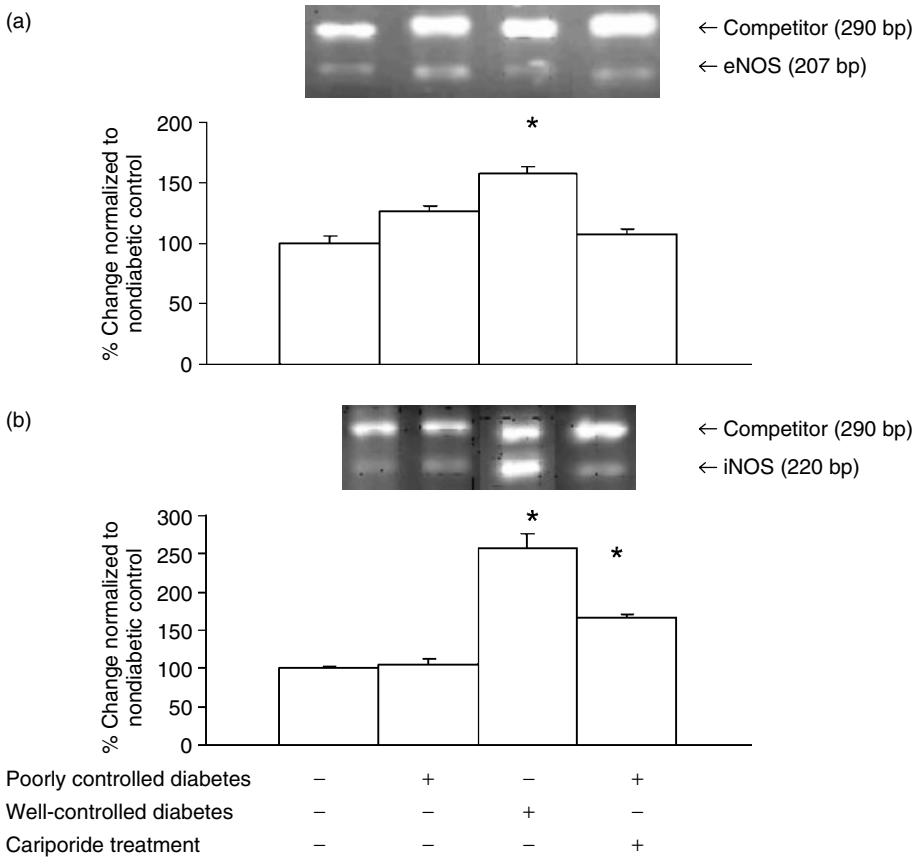

Figure 4. eNOS and iNOS mRNA expression. Quantitative analysis of (a) eNOS and (b) iNOS mRNA expression show no effect of diabetes on the transcription level. However, good glycemic control with increased insulin upregulated eNOS mRNA. Treatment of diabetic animals with cariporide or improved glycemic control with increased insulin levels did upregulate iNOS expression. The upper panels of parts (a) and (b) are representative gel pictures obtained from competitive RT PCR. Similar mRNA expression was seen with real-time PCR analysis. (∗ significantly different from nondiabetic control. $n = 5$ for all groups)

NHE-1 mRNA expression [46,47]. Similarly, vascular smooth muscle cells cultured in high glucose show increased NHE-1 mRNA expression [40]. On the other hand, it appears that these changes may be organ specific. In the heart of streptozotocin (STZ)-induced diabetic rats, we did not find an alteration of NHE-1 mRNA during short-term diabetes [18]. In contrast, a recent report by Feuvray *et al*. suggests that NHE activity is increased in cardiomyocytes isolated from a type 2 diabetes animal model [48].

This report further demonstrates that improved glycemic control leads to an improvement of RI, which was associated with an increase in both eNOS and iNOS mRNA expression. It is to be noted that we were unable to achieve a euglycemic level and ET mRNA remained elevated. However, relative lowering of blood glucose as well as higher insulin levels may have led to increased NOS expression and vasodilatation counteracting the effects of ETs. Previous work has demonstrated an insulin-dependent increase in both ET and NOS expressions [49–51]. In spite of increased ET expression, the increased NOS expression may have caused a vasodilatory effect and improved the RI. Interestingly, cariporide treatment also increased iNOS mRNA expression.

Our data suggests that in diabetes, NHE-1 is involved in the regulation of both ETs and NOS. We have previously demonstrated a relationship between NHE-1 and ET-1 expression in the heart due to diabetes [18]. Further experiments are required to elucidate whether the regulation occurs directly through protein–protein interactions or indirectly by changes in intracellular H^+, Na^+, or Ca^{2+} concentrations [52,53]. Conceptually, NHE-1 inhibition may lead to PKC inhibition or attenuated activation via reduced Na^+/Ca^{2+} exchanger and reduced Ca^{2+} [54–56]. A reduction in PKC activation via NHE blockade leads to diminished ET expression [57,58]. In addition, NHE-1 inhibition may modulate endothelin-converting enzyme activity by disrupting actin networks [59–61]. Reduced ET mRNA levels may cause an NOS upregulation counteracting an ET-mediated increased RI. However, these notions require direct confirmation. Similarly, in good glucose controlled diabetic animals, increased NOS expression appears to be the main mechanism leading to the prevention of diabetes-induced, ET-mediated increased RI. This phenomenon may be in part due to the reciprocal relationship that exists between ET and NO [62]. Because blood glucose levels were not reduced to the level of nondiabetic control animals, we believe some of the effects of hyperglycemia persisted. Along with increased NHE-1 mNRA, both ET-1 and ET-3 levels remained higher in these animals, similar to the level of animals with poorly controlled

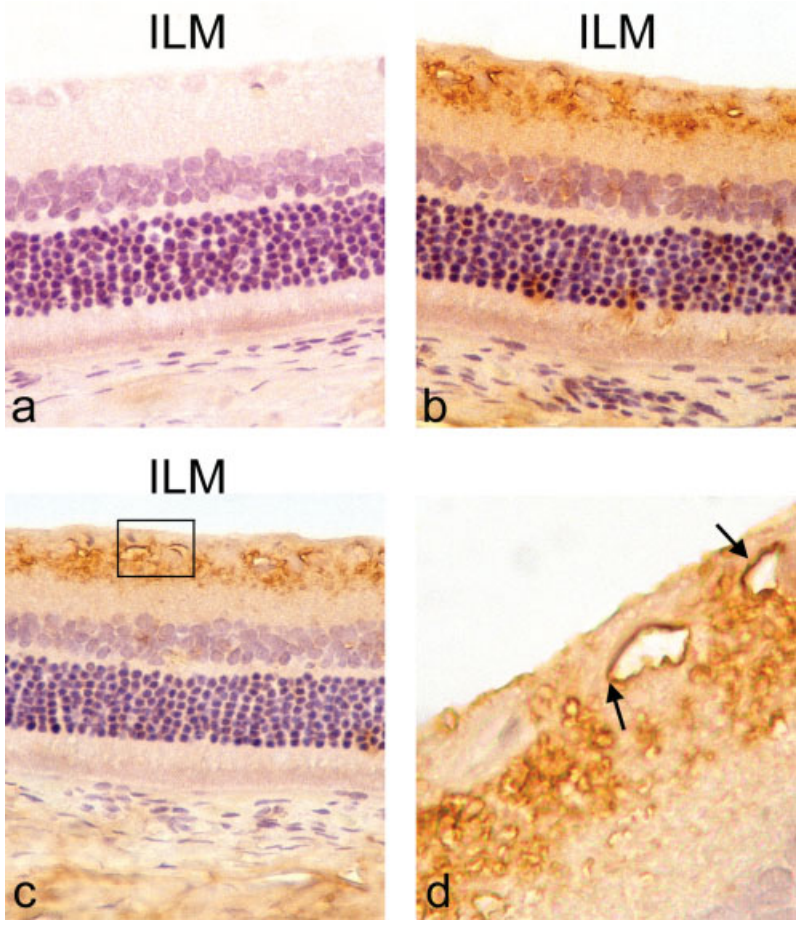

Figure 5. Immunocytochemical analysis of retinal NHE-1. (a) Negative control. (b) NHE-1 immunostain of the retina from poorly controlled diabetic animals. (c) NHE-1 immunostain from the retina of nondiabetic control animals. (d) Higher magnification of the enclosed area of (c) demonstrating with arrows the NHE-1 localization within the endothelial cells of a capillary. (ILM = inner limiting membrane. Magnification of (a), (b), (c) = ×225, magnification of (d) = ×975)

diabetes. It is possible that ET-1 and ET-3 mRNA levels might have reached the upper limit and did not increase further in spite of higher NHE-1 mRNA expression. On the other hand, high systemic insulin levels may have further led to NOS and NHE-1 upregulation, since insulin is a known stimulator of these transcripts [41,49]. As expected, owing to the inhibitory effect of cariporide with respect to NHE-1 activity and not NHE-1 gene transcription, cariporide did not decrease NHE-1 mRNA expression.

In summary, the present data suggests that NHE-1 may regulate retinal ET and NOS expression. NHE-1 inhibition may improve blood flow by modulating such vasoactive factors. Whether the effect is by direct protein–protein interaction or through an indirect mechanism like attenuated PKC activation remains to be investigated.

Acknowledgments

We would like to recognize the work of Mr Yousef Pashei Barbin in preparing the innmunohistochemistry for this manuscript. The authors wish to thank the Canadian Diabetes Association (in memory of Margaret Francis), The Canadian Institute of Health Research (MOP 438411) and the Lawson Health Research Institute (Internal Research Fund) for their continued funding support. Dr Karmazyn is an Ontario Heart and Stroke Foundation Career Investigator.

References

1. Wakabayashi S, Shigekawa M, Pouyssegur J. Molecular physiology of vertebrate Na+/H+ exchangers. *Physiol Rev* 1997; **77**: 51–74.
2. Numata M, Orlowski J. Molecular cloning and characterization of a novel (Na+, K+)/H+ exchanger localized to the trans-Golgi network. *J Biol Chem* 2001; **276**: 17387–17394.
3. Numata M, Petrecca K, Lake N, Orlowski J. Identification of a mitochondrial Na+/H+ exchanger. *J Biol Chem* 1998; **273**: 6951–6959.
4. Karmazyn M, Gan XT, Humphreys RA, Yoshida H, Kusumoto K. The myocardial Na(+)-H(+) exchange: structure, regulation, and its role in heart disease. *Circ Res* 1999; **85**: 777–786.
5. Counillon L, Pouyssegur J. The expanding family of eucaryotic Na(+)/H(+) exchangers. *J Biol Chem* 2000; **275**: 1–4.
6. Siczkowski M, Ng LL. Phorbol ester activation of the rat vascular myocyte Na(+)-H(+) exchanger isoform 1. *Hypertension* 1996; **27**: 859–866.
7. Williams B, Howard RL. Glucose-induced changes in Na+/H+ antiport activity and gene expression in cultured smooth muscle cells. Role of protein kinase C. *J Clin Invest* 1994; **93**: 2623–2631.

8. Putney LK, Denker SP, Barber DL. The changing face of the Na+/H+ exchanger, NHE1: structure, regulation, and cellular actions. *Annu Rev Pharmacol Toxicol* 2002; **42**: 527–552.
9. Sheetz MJ, King GL. Molecular understanding of hyperglycemia's adverse effects for diabetic complications. *JAMA* 2002; **288**: 2579–2588.
10. Brownlee M. Biochemistry and molecular cell biology of diabetic complications. *Nature* 2001; **414**: 813–820.
11. Chakrabarti S, Cukiernik M, Hileeto D, Evans T, Chen S. Role of vasoactive factors in the pathogenesis of early changes in diabetic retinopathy. *Diabetes Metab Res Rev* 2000; **16**: 393–407.
12. Candido R, Allen TJ. Haemodynamics in microvascular complications in type 1 diabetes. *Diabetes Metab Res Rev* 2002; **18**: 286–304.
13. Evans T, Xi DD, Mukherjee K, Downey D, Chakrabarti S. Endothelins, their receptors, and retinal vascular dysfunction in galactose-fed rats. *Diabetes Res Clin Pract* 2000; **48**: 75–85.
14. Deng D, Evans T, Mukherjee K, Downey D, Chakrabarti S. Diabetes-induced vascular dysfunction in the retina: role of endothelins. *Diabetologia* 1999; **42**: 1228–1234.
15. Evans T, Deng DX, Chen S, Chakrabarti S. Endothelin receptor blockade prevents augmented extracellular matrix component mRNA expression and capillary basement membrane thickening in the retina of diabetic and galactose-fed rats. *Diabetes* 2000; **49**: 662–666.
16. Chen S, Evans T, Deng D, Cukiernik M, Chakrabarti S. Hyperhexosemia induced functional and structural changes in the kidneys: role of endothelins. *Nephron* 2002; **90**: 86–94.
17. Chen S, Mukherjee S, Chakraborty C, Chakrabarti S. High glucose-induced, endothelin-dependent fibronectin synthesis is mediated via NF-kappa B and AP-1. *Am J Physiol Cell Physiol* 2003; **284**: C263–C272.
18. Hileeto D, Cukiernik M, Mukherjee S, *et al*. Contributions of endothelin-1 and sodium hydrogen exchanger-1 in the diabetic myocardium. *Diabetes Metab Res Rev* 2002; **18**: 386–394.
19. Gan XT, Chakrabarti S, Karmazyn M. Modulation of Na+/H+ exchange isoform 1 mRNA expression in isolated rat hearts. *Am J Physiol* 1999; **277**: H993–H998.
20. Woo SH, Lee CO. Effects of endothelin-1 on Ca2+ signaling in guinea-pig ventricular myocytes: role of protein kinase C. *J Mol Cell Cardiol* 1999; **31**: 631–643.
21. Wu ML, Tseng YZ. The modulatory effects of endothelin-1, carbachol and isoprenaline upon Na(+)-H+ exchange in dog cardiac Purkinje fibres. *J Physiol* 1993; **471**: 583–597.
22. Ito N, Kagaya Y, Weinberg EO, Barry WH, Lorell BH. Endothelin and angiotensin II stimulation of Na+-H+ exchange is impaired in cardiac hypertrophy. *J Clin Invest* 1997; **99**: 125–135.
23. Khandoudi N, Ho J, Karmazyn M. Role of Na(+)-H+ exchange in mediating effects of endothelin-1 on normal and ischemic/reperfused hearts. *Circ Res* 1994; **75**: 369–378.
24. Podesta F, Meregalli G, Ghelardi R, *et al*. Low Ca(2+) pump activity in diabetic nephropathy. *Am J Kidney Dis* 2001; **38**: 465–472.
25. Ganz MB, Hawkins K, Reilly RF. High glucose induces the activity and expression of Na(+)/H(+) exchange in glomerular mesangial cells. *Am J Physiol Renal Physiol* 2000; **278**: F91–F96.
26. Koren W, Koldanov R, Pronin VS, *et al*. Enhanced erythrocyte Na+/H+ exchange predicts diabetic nephropathy in patients with IDDM. *Diabetologia* 1998; **41**: 201–205.
27. Kenyon E, Maminishkis A, Joseph DP, Miller SS. Apical and basolateral membrane mechanisms that regulate pHi in bovine retinal pigment epithelium. *Am J Physiol* 1997; **273**: C456–C472.
28. Katz BJ, Oakley B. Evidence for Na+/H+ exchange in vertebrate rod photoreceptors. *Exp Eye Res* 1990; **51**: 199–207.
29. Zadunaisky JA, Kinne-Saffran E, Kinne R. A Na/H exchange mechanism in apical membrane vesicles of the retinal pigment epithelium. *Invest Ophthalmol Vis Sci* 1989; **30**: 2332–2340.
30. Mather K, Anderson TJ, Verma S. Insulin action in the vasculature: physiology and pathophysiology. *J Vasc Res* 2001; **38**: 415–422.
31. Ceolotto G, Conlin P, Clari G, Semplicini A, Canessa M. Protein kinase C and insulin regulation of red blood cell Na+/H+ exchange. *Am J Physiol* 1997; **272**: C818–C826.
32. Incerpi S, Rizvi SI, De Vito P, Luly P. Insulin stimulation of Na/H antiport in L-6 cells: a different mechanism in myoblasts and myotubes. *J Cell Physiol* 1997; **171**: 235–242.
33. Sauvage M, Maziere P, Fathallah H, Giraud F. Insulin stimulates NHE1 activity by sequential activation of phosphatidylinositol 3-kinase and protein kinase C zeta in human erythrocytes. *Eur J Biochem* 2000; **267**: 955–962.
34. Scholz W, Albus U, Counillon L, *et al*. Protective effects of HOE642, a selective sodium-hydrogen exchange subtype 1 inhibitor, on cardiac ischaemia and reperfusion. *Cardiovasc Res* 1995; **29**: 260–268.
35. Counillon L, Touret N, Bidet M, *et al*. Na+/H+ and Cl-/HCO3- antiporters of bovine pigmented ciliary epithelial cells. *Pflugers Arch* 2000; **440**: 667–678.
36. Harvitt DM, Bonanno JA. pH dependence of corneal oxygen consumption. *Invest Ophthalmol Vis Sci* 1998; **39**: 2778–2781.
37. Wu X, Torres-zamorano V, Yang H, Reinach PS. ETA receptor mediated inhibition of intracellular pH regulation in cultured bovine corneal epithelial cells. *Exp Eye Res* 1998; **66**: 699–708.
38. Reinach P, Ganapathy V, Torres-zamorano V. A Na : H exchanger subtype mediates volume regulation in bovine corneal epithelial cells. *Adv Exp Med Biol* 1994; **350**: 105–110.
39. Zerbini G, Roth T, Podesta F, *et al*. Activity and expression of the Na+/H+ exchanger in human endothelial cells cultured in high glucose. *Diabetologia* 1995; **38**: 785–791.
40. Hannan KM, Little PJ. Mechanisms regulating the vascular smooth muscle Na/H exchanger (NHE-1) in diabetes. *Biochem Cell Biol* 1998; **76**: 751–759.
41. Besson P, Fernandez-Rachubinski F, Yang W, Fliegel L. Regulation of Na+/H+ exchanger gene expression: mitogenic stimulation increases NHE1 promoter activity. *Am J Physiol* 1998; **274**: C831–C839.
42. Sabri A, Byron KL, Samarel AM, Bell J, Lucchesi PA. Hydrogen peroxide activates mitogen-activated protein kinases and Na+-H+ exchange in neonatal rat cardiac myocytes. *Circ Res* 1998; **82**: 1053–1062.
43. el Seifi S, Freiberg JM, Kinsella J, Cheng L, Sacktor B. Na+-H+ exchange and Na+-dependent transport systems in streptozotocin diabetic rat kidneys. *Am J Physiol* 1987; **252**: R40–R47.
44. Trevisan R, Viberti G. Sodium-hydrogen antiporter: its possible role in the genesis of diabetic nephropathy. *Nephrol Dial Transplant* 1997; **12**: 643–645.
45. Rutherford P, Pizzonia J, Abu-Alfa A, Biemesderfer D, Reilly R, Aronson P. Sodium-hydrogen exchange isoform expression in blood cells: implications for studies in diabetes mellitus. *Exp Clin Endocrinol Diabetes* 1997; **105**(Suppl. 2): 13–16.
46. Standley PR, Zhang F, Zayas RM, *et al*. IGF-I regulation of Na(+)-K(+)-ATPase in rat arterial smooth muscle. *Am J Physiol* 1997; **273**: E113–E121.
47. Kuriyama S, Tokudome G, Tomonari H, *et al*. Differential regulation of cation transport of vascular smooth muscle cells in a high glucose concentration milieu. *Diabetes Res Clin Pract* 1994; **24**: 77–84.
48. Feuvray D. The paradoxical role of Na+/H+ exchanger in the diabetic heart. In *The Sodium-Hydrogen Exchanger. From Molecule to its Role in Disease*, Karmazyn M, Aykiran L, Fliegel L (eds). Kluwer Academic Publishers: Dordrecht/Boston/London, 2003; 149–158.
49. Ribiere C, Jaubert AM, Sabourault D, Lacasa D, Giudicelli Y. Insulin stimulates nitric oxide production in rat adipocytes. *Biochem Biophys Res Commun* 2002; **291**: 394–399.
50. Jiang ZY, Zhou QL, Chatterjee A, *et al*. Endothelin-1 modulates insulin signaling through phosphatidylinositol 3-kinase pathway in vascular smooth muscle cells. *Diabetes* 1999; **48**: 1120–1130.
51. Eringa EC, Stehouwer CD, Merlijn T, Westerhof N, Sipkema P. Physiological concentrations of insulin induce endothelin-mediated vasoconstriction during inhibition of NOS or PI3-kinase in skeletal muscle arterioles. *Cardiovasc Res* 2002; **56**: 464–471.
52. Hartmann M, Decking UK. Blocking Na(+)-H+ exchange by cariporide reduces Na(+)-overload in ischemia and is cardioprotective. *J Mol Cell Cardiol* 1999; **31**: 1985–1995.
53. Stromer H, de Groot MC, Horn M, *et al*. Na(+)/H(+) exchange inhibition with HOE642 improves postischemic recovery due to attenuation of Ca(2+) overload and prolonged acidosis on reperfusion. *Circulation* 2000; **101**: 2749–2755.
54. Park CO, Xiao XH, Allen DG. Changes in intracellular Na+ and pH in rat heart during ischemia: role of Na+/H+ exchanger. *Am J Physiol* 1999; **276**: H1581–H1590.
55. Greene DA, Sima AA, Stevens MJ, Feldman EL, Lattimer SA. Complications: neuropathy, pathogenetic considerations. *Diabetes Care* 1992; **15**: 1902–1925.

56. Tani M, Neely JR. Role of intracellular Na+ in Ca2+ overload and depressed recovery of ventricular function of reperfused ischemic rat hearts. Possible involvement of H+-Na+ and Na+-Ca2+ exchange. *Circ Res* 1989; **65**: 1045–1056.
57. Ishii H, Koya D, King GL. Protein kinase C activation and its role in the development of vascular complications in diabetes mellitus. *J Mol Med* 1998; **76**: 21–31.
58. Chen S, Apostolova MD, Cherian MG, Chakrabarti S. Interaction of endothelin-1 with vasoactive factors in mediating glucose-induced increased permeability in endothelial cells. *Lab Invest* 2000; **80**: 1311–1321.
59. Barnes K, Turner AJ. Endothelin converting enzyme is located on alpha-actin filaments in smooth muscle cells. *Cardiovasc Res* 1999; **42**: 814–822.
60. Denker SP, Huang DC, Orlowski J, Furthmayr H, Barber DL. Direct binding of the Na–H exchanger NHE1 to ERM proteins regulates the cortical cytoskeleton and cell shape independently of H(+) translocation. *Mol Cell* 2000; **6**: 1425–1436.
61. Tominaga T, Barber DL. Na-H exchange acts downstream of RhoA to regulate integrin-induced cell adhesion and spreading. *Mol Biol Cell* 1998; **9**: 2287–2303.
62. Honing ML, Morrison PJ, Banga JD, Stroes ES, Rabelink TJ. Nitric oxide availability in diabetes mellitus. *Diabetes Metab Rev* 1998; **14**: 241–249.

